Switching strategies for DTC on asymmetric converters

José Restrepo, José M. Aller, Víctor M Guzmán, María I. Giménez and Julio C. Viola
UNIVERSIDAD SIMÓN BOLÍVAR
Departamento de Electrónica y Circuitos
Valle de Sartenejas, Baruta, Edo. Miranda
Caracas, Venezuela
Phone: +58 (212) 906-4012
E-Mail: restrepo@usb.ve
URL: http://www.usb.ve

Acknowledgments

The authors would like to thank the Dean of research and development at the Simón Bolívar University for the financial support to this work.

Keywords

<<Direct torque and flux control>>, <<Converter control>>, <<Induction motor>>.

Abstract

In this work the application of additional switching states for the asymmetric converter is studied for its use in direct torque control. The proposed algorithm makes use of previously discarded states, that can increase the operational range of asymmetric converters by increasing the total number of switching states available for control. The proposed algorithm was simulated while controlling an induction machine and compared with the classical direct torque control.

Introduction

Asymmetric converters are usually found in the power stage of highly non-linear machines such as stepper-motors and switch reluctance motors. Due to its structure these converters present more switching states than conventional inverters. However few control strategies exploiting the presence of those additional states have been developed. A control scheme using the Direct Torque Control (DTC) philosophy was presented in [1], where flux and torque are directly controlled through the stator voltage. This scheme offers the DTC advantages in Asymmetric converters, limiting flux and torque ripples to precalculated hysteresis bands. The DTC scheme has many advantages over conventional control techniques, such as a fast dynamic response, simplicity and robustness, but it has the disadvantage of a variable power stage commutating frequency, and inherent ripples in stator flux, current and generated motor torque.
In this work the capability of using previously discarded states is investigated in the development of a classical direct torque control algorithm. To investigate the usefulness of the method, and for comparison purposes, the converter operation is simulated on an induction machine with independent stator windings.

Asymmetric converter

Fig. 1 shows the diagram of the three phase asymmetric converter used in this work. Since the converter have six independent and controlled switching devices, there are 64 possible switching states, and in this

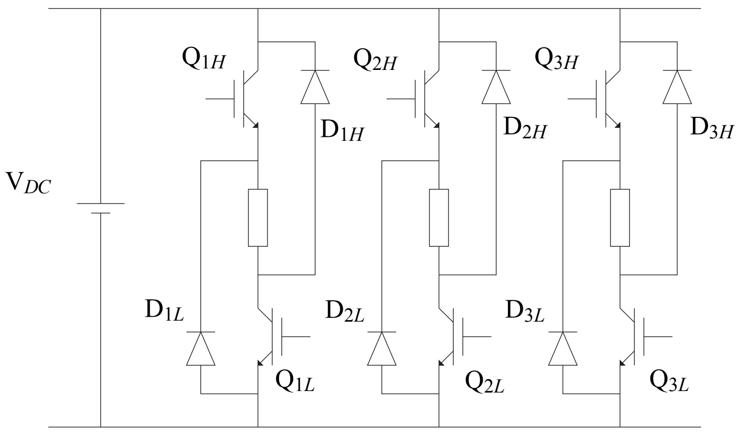

Fig. 1: Circuit diagram of the three phase asymmetric converter.

case all of those possible states are valid states. This in contrast to the conventional three phase converter which has 37 forbidden states due to short circuit of the DC link, 19 unused states when both switches on a branch are turned off, and only eight valid states, two of which correspond to space vector zero. In the standard three phase inverter the 19 unused states during regeneration have a corresponding valid state, so no additional space vectors can be obtained from these unused states. The asymmetric converter switching states can be categorized in five different sets, according to the space vectors produced. In the asymmetric converter each branch have the following there possible states: State $\{1\}$, obtained when both switches are turned on, state $\{0\}$, obtained when one switch is turned on and the other is turned off and state {-1} obtained when both switches are turned off and the current in the branch is larger than zero.
The voltage space vectors produced by the converter are obtained using the following expression.

$$\vec{v}_s = \sqrt{\frac{2}{3}} V_{DC} \begin{bmatrix} 1 & e^{j2\pi/3} & e^{j4\pi/3} \end{bmatrix} \cdot [S_{ph1} \;\; S_{ph2} \;\; S_{ph3}] \tag{1}$$

where S_{ph1}, S_{ph2}, S_{ph3} are the switching states of each branch.
Using (1) the following set of space vectors are obtained: A first set made of three zero magnitude space vectors {(-1,-1,-1), (0,0,0), (1,1,1)}. Next, two sets of six space vectors with small magnitude, one set obtained with combination of states $\{0\}$ and $\{1\}$ in each converter branch and the other set obtained with combination of states $\{0\}$ and $\{-1\}$ in each converter branch. It follows a medium size space vectors obtained with one branch in $\{0\}$, other in $\{1\}$ and the other in $\{-1\}$. Finally, a set of large space vectors obtained with the combination of $\{-1\}$ and $\{1\}$ in each converter branch. Fig. 2 shows a representation of the different space vector sets.

DTC algorithm

The conventional DTC algorithm was proposed by Takahashi et al. [2], uses a calculator block to obtain the computed values for the instantaneous stator flux and electric torque in the machine. The calculated torque and flux values are compared with the corresponding reference values and their error signals are fed to hysteresis comparators. The output of these comparators together with the information of the angular flux location are used to address the switching table. In [2] the stator flux space vector plane is divided in six regions and Table I shows the corresponding look-up table for the classical DTC algorithm. The stator flux linkage can be derived by integrating the electromotive force in the stator winding using the following expression.

$$\vec{\Psi}_s = \int \left(\vec{v}_s - R_s \vec{i}_s \right) dt \tag{2}$$

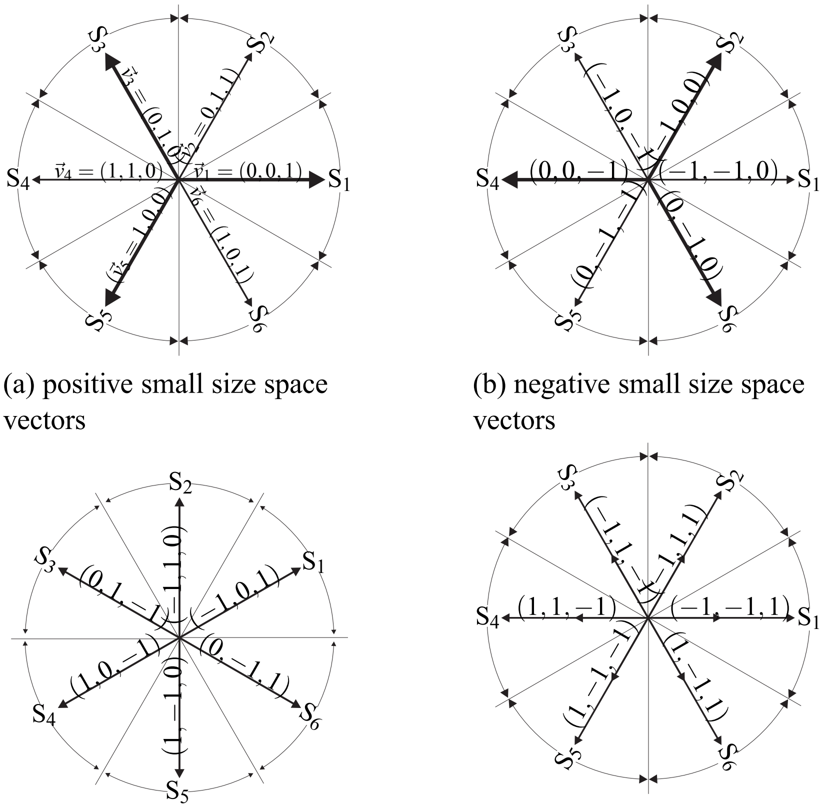

(a) positive small size space vectors

(b) negative small size space vectors

(c) medium size space vectors

(d) large size space vectors

Fig. 2: Set of space vectors for the asymmetric converter.

The electric torque is obtained multiplying the stator flux linkage and the stator current space vectors.

$$\tau_e = \vec{\Psi}_s \times \vec{i}_s \tag{3}$$

The electric torque and the stator linkage flux are adjusted by the DTC algorithm applying the stator voltage space vector that compensates both errors. In the case of the conventional converter there are only five possible stator voltage space vectors available in each region for the compensation. In the asymmetric converter there are many more available choices. The optimum switching table for equal size space vectors with $\pi/3$ phase lag between them, used in the classical DTC algorithm, can still be applied in this general case.

As mentioned previously, there are four set of space vectors of equal magnitude that could be manipulated to perform the DTC over the asymmetric converter. In [1] the algorithm is applied to the control of a switched reluctance machine (SRM) using the medium size vectors shown in Fig. 2c. In this work the analysis is expanded to include the use of the set of small vectors shown in Figs. 2a-b, but applied to the asymmetric converter feeding an induction machine. For the simulations the induction machine was modeled in the natural abc coordinates using the following equations.

$$[\vec{v}] = [R]\left[\vec{i}\right] + [L(\theta)]\,p\left[\vec{i}\right] + \dot{\theta}\,[\tau(\theta)]\left[\vec{i}\right] \tag{4}$$

where

$$[\vec{v}] = \begin{bmatrix} [\vec{v}_s] \\ [\vec{v}_r] \end{bmatrix} = \begin{bmatrix} [v_{sa}\ v_{sb}\ v_{sc}]^t \\ [v_{ra}\ v_{rb}\ v_{rc}]^t \end{bmatrix}; \quad [\vec{i}] = \begin{bmatrix} [\vec{i}_s] \\ [\vec{i}_r] \end{bmatrix} = \begin{bmatrix} [i_{sa}\ i_{sb}\ i_{sc}]^t \\ [i_{ra}\ i_{rb}\ i_{rc}]^t \end{bmatrix}$$

$$[R] = \begin{bmatrix} R_s\,[I] & [0] \\ [0] & R_r\,[I] \end{bmatrix}; \quad [L(\theta)] = \begin{bmatrix} L_{\sigma s}\,[I] + L_{ms}\,[S] & L_{sr}\,[C(\theta)] \\ L_{sr}\,[C(\theta)]^t & L_{\sigma r}\,[I] + L_{mr}\,[S] \end{bmatrix}$$

Table I: **DTC space vector selection**

C_{τ_e}	C_{Ψ_s}	S(1)	S(2)	S(3)	S(4)	S(5)	S(6)
-1	-1	$\vec{v}_5$	$\vec{v}_6$	$\vec{v}_1$	$\vec{v}_2$	$\vec{v}_3$	$\vec{v}_4$
0	-1	$\vec{v}_0$	$\vec{v}_7$	$\vec{v}_0$	$\vec{v}_7$	$\vec{v}_0$	$\vec{v}_7$
1	-1	$\vec{v}_3$	$\vec{v}_4$	$\vec{v}_5$	$\vec{v}_6$	$\vec{v}_1$	$\vec{v}_2$
-1	1	$\vec{v}_6$	$\vec{v}_1$	$\vec{v}_2$	$\vec{v}_3$	$\vec{v}_4$	$\vec{v}_5$
0	1	$\vec{v}_7$	$\vec{v}_0$	$\vec{v}_7$	$\vec{v}_0$	$\vec{v}_7$	$\vec{v}_0$
1	1	$\vec{v}_2$	$\vec{v}_3$	$\vec{v}_4$	$\vec{v}_5$	$\vec{v}_6$	$\vec{v}_1$

$$[\tau(\theta)] = \begin{bmatrix} [0] & L_{sr}\frac{d}{d\theta}[C(\theta)] \\ L_{sr}\frac{d}{d\theta}[C(\theta)]^t & [0] \end{bmatrix}$$

$$[I] = \begin{bmatrix} 1 & 0 & 0 \\ 0 & 1 & 0 \\ 0 & 0 & 1 \end{bmatrix}; \quad [0] = \begin{bmatrix} 0 & 0 & 0 \\ 0 & 0 & 0 \\ 0 & 0 & 0 \end{bmatrix}; \quad [S] = \begin{bmatrix} 1 & -\frac{1}{2} & -\frac{1}{2} \\ -\frac{1}{2} & 1 & -\frac{1}{2} \\ -\frac{1}{2} & -\frac{1}{2} & 1 \end{bmatrix}$$

$$[C(\theta)] = \begin{bmatrix} \cos(\theta) & \cos(\theta+\frac{2\pi}{3}) & \cos(\theta-\frac{2\pi}{3}) \\ \cos(\theta-\frac{2\pi}{3}) & \cos(\theta) & \cos(\theta+\frac{2\pi}{3}) \\ \cos(\theta+\frac{2\pi}{3}) & \cos(\theta-\frac{2\pi}{3}) & \cos(\theta) \end{bmatrix}$$

$$\frac{d}{d\theta}[C(\theta)] = -\begin{bmatrix} \sin(\theta) & \sin(\theta+\frac{2\pi}{3}) & \sin(\theta-\frac{2\pi}{3}) \\ \sin(\theta-\frac{2\pi}{3}) & \sin(\theta) & \sin(\theta+\frac{2\pi}{3}) \\ \sin(\theta+\frac{2\pi}{3}) & \sin(\theta-\frac{2\pi}{3}) & \sin(\theta) \end{bmatrix}$$

and,

R_s, R_r	Stator and rotor resistance.
$L_{\sigma s}, L_{\sigma_r}$	Stator and rotor leakage inductance.
L_{ms}, L_{mr}	Stator and rotor mutual inductance.
L_{sr}	Mutual stator-rotor coupling inductance.

The block diagram for the classical DTC algorithm is shown in Fig. 3 and the same control block can be used together with Table I with the asymmetric converter, but the sector selection will depend on the set of vectors used for the implementation of the algorithm, as shown in Fig. 2. Controlling the asymmetric converter, using the positive small vectors or the negative small vectors alone, will require the adjustment of the zero sequence component in the stator voltages for proper operation. For the positive small vectors, a negative value of the zero sequence component is required to reduce the DC component in the stator currents, while for the negative small vectors a positive value of the zero sequence component will be required to provided enough current to produce the regenerative vectors.

In [3][4][5] the medium size set of voltage space vectors is used for the DTC algorithm, and considered as the only set of space vectors allowed by the controller. However, since this medium size set of vectors can be synthesized with the positive and negative set of vectors, the proposed algorithm presented in this paper uses a combination of this two sets for the application of the DTC algorithm, increasing in this way the amount of possible states usable by the controller. In the proposed algorithm the main idea is to guarantee enough energy in the phase leakage inductances to maintain the regenerative states when a $\{-1\}$ state is required. To attain this, the algorithm tries to use the negative set of vectors when ever is possible, and the positive set of vectors if the conditions are not appropriate for the former. So, if the current in any phase falls below a pre-selected minimum value, the algorithm will synthesize the required voltage space vector with the positive set, otherwise it will use the negative set.

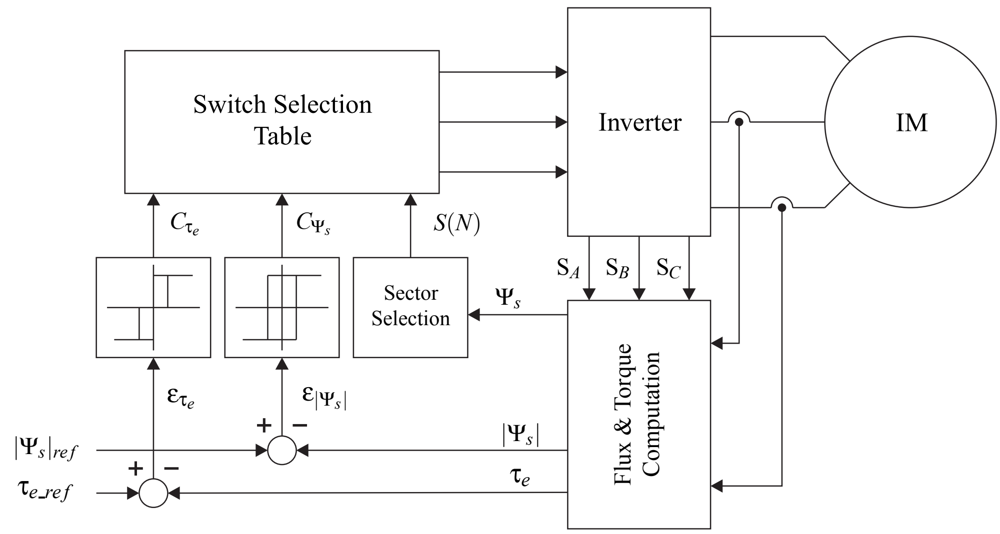

Fig. 3: Block diagram of the classical direct torque controller.

Table II: **Electrical parameters for the induction machine**

Model	SKI80-43
HP	1 HP
Voltage	220V/380V
Current	3.3A/1.92A
Nominal speed	4400 rpm
frequency	50 Hz
Stator resistance	8.2Ω
Rotor resistance	10.58Ω
Stator inductance	0.866 H
Rotor inductance	0.866 H
Mutual inductance	0.83 H

Simulations and experimental results

As mentioned previously, for the simulation, an induction machine modeled in real a, b, c coordinates was used as the load for the asymmetric converter. The system was simulated by programming the induction machine equations and the DTC vector selection algorithm using C language, running on an Analog Devices digital signal processor (ADSP-21369)[6]. The differential equations modeling the induction machine were solved by using a standard fixed step fourth order Runge-Kutta Ordinary Differential Equations (ODE) integrator, the integration steps during the control cycle were obtained by simulating the PWM-SVM modulator. The simulation is simplified by using a fixed voltage DC link; the electrical parameters for the induction machine are given in Table II. For the experimental part, the DTC algorithm using medium size set of vectors was implemented on a custom build floating point DSP based test-rig (ADSP-21364 at 320 MHz). The power stage uses six 27A, 600V, IGBTs with one 2200 μF 450 V capacitor in the DC link. The switching signals where synthesized with an on-chip PWM operating at 10 kHz. The sampling frequency was synchronized with the beginning of a PWM cycle. Fig. 4 shows the actual test rig used for the simulation and experimental tests.

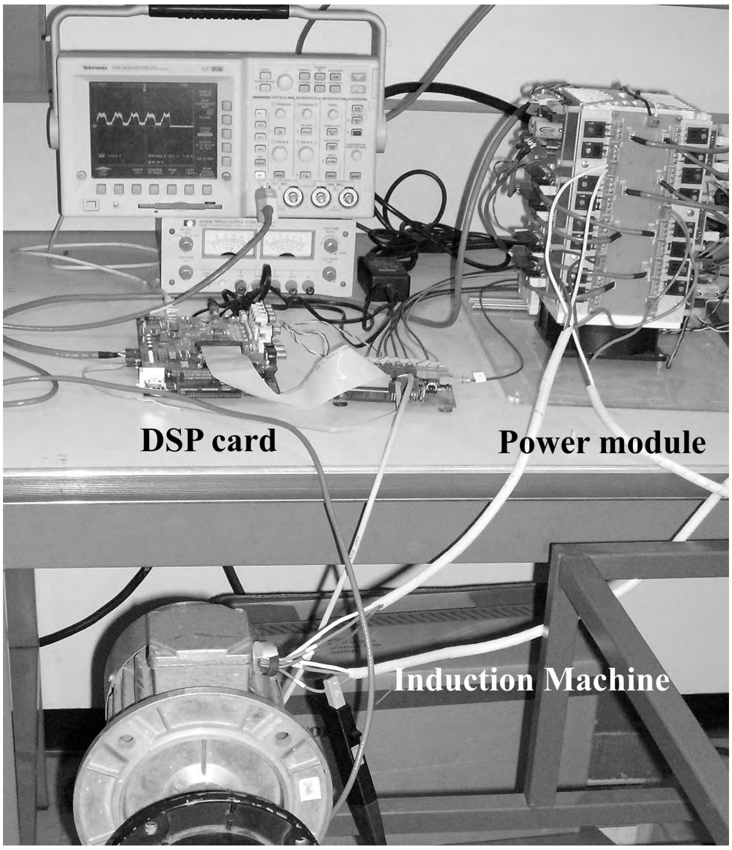

Fig. 4: Test rig used for the simulation and experimental tests.

Initially the controller was simulated for the DTC algorithm using the medium size set of vectors, reported in [3] as the only set usable for DTC in the asymmetric converter. Next an additional set of states were tested using the positive and negative small size sets of vectors. Fig. 5a shows the flux evolution while using the classical DTC algorithm with a flux reference of 0.7 Wb, and Figs. 5b and 5c show the current in one of the windings and the total electric torque. The results show that the flux is maintained within the selected hysteresis band, and the current and torque have the typical ripple present in DTC algorithms.

The results for the simulation of the proposed method are shown in Figs. 6a- 6c. In Fig. 6a the current in the windings is kept positive by switching between the two set of small voltage space vectors, and this control action provides enough zero component in the stator windings without the need to add any additional component to the phase voltages. Fig. 6b shows the evolution of the stator flux, following a circular trajectory similar to the one obtained with the medium size set of vectors and Fig. 6c shows the torque produced by the converter when the algorithm uses the proposed algorithm; in this case the torque reference is maintained at about 1.3 N.m while the rotational speed is below the reference speed (80 rad/s) and goes down to 0.1 N.m when the speed is above the reference speed.

Fig. 7a shows the measured current in phase ‘a’ when the DTC algorithm for the asymmetric converter uses the medium size voltage space vectors. An additional control loop is added to the system to limit the phase currents magnitude. This is achieved by reducing the voltage space vector if the current is large. The corresponding evolution of the experimental values of stator flux and electric torque are depicted in Figs. 7b and 7c. The results are similar to those obtained in the simulation, and the differences can be associated to the non linearities in the induction machine and in the power stage.

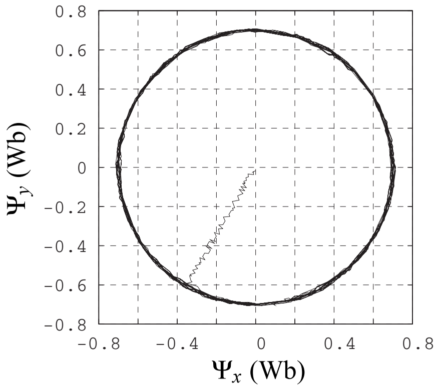

(a) Simulated stator flux.

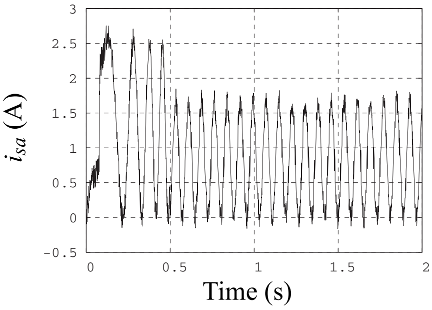

(b) Simulated phase ‘a’ current.

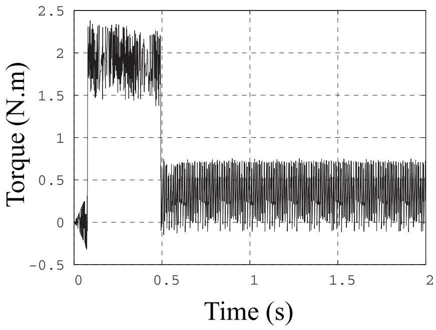

(c) Simulated electric torque.

Fig. 5: Simulations for the DTC with medium size space vectors.

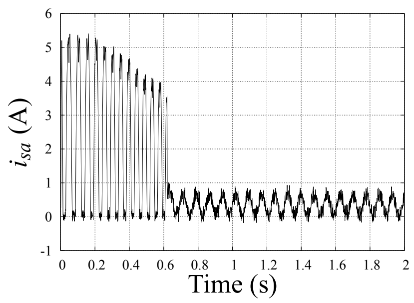

(a) Simulated phase ‘a’ current.

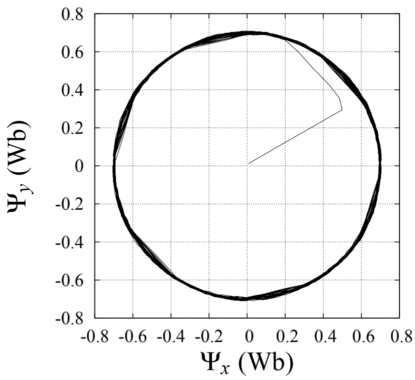

(b) Simulated stator flux.

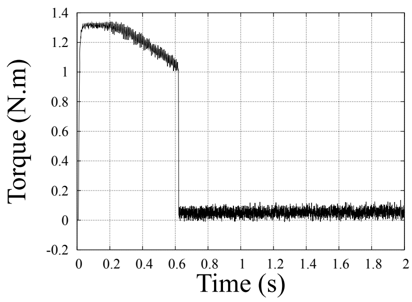

(c) Simulated electric torque.

Fig. 6: Simulations for the proposed DTC algorithm.

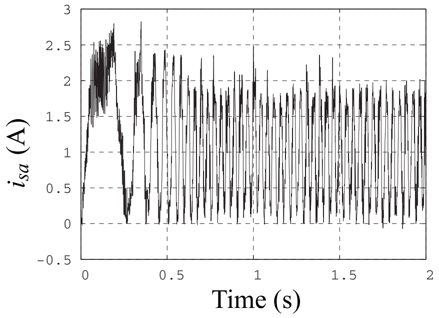

(a) Experimental phase 'a' current.

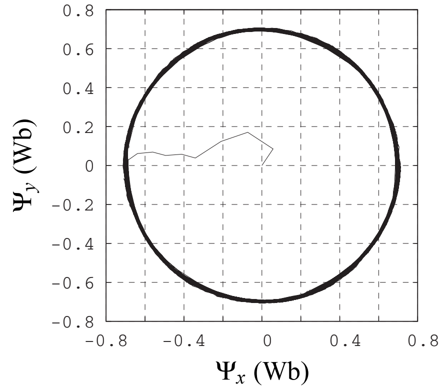

(b) Experimental stator flux.

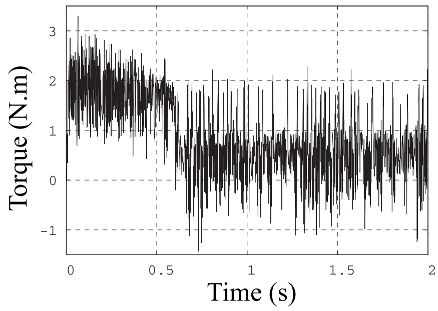

(c) Experimental electric torque.

Fig. 7: Experimental results for the DTC with medium size space vectors.

Conclusion

The results presented in this paper show that additional switching states can be employed for the implementation of a DTC algorithm in asymmetric converters. The additional states can be used to add more entries to the switching table, and a reduction of the current and torque ripple is obtained with the use of the additional states presented in this work. Simulation results for the medium size set of vectors are shown to serve as a reference for comparison with the results obtained when using the proposed algorithm. Experimental results for the proposed algorithm will be included in a future work.

References

[1] A. D. Cheok and P. H. Hoon, "A new torque control method for switched reluctance motor drives," in *26th Anual conference of the IEEE Industrial Electronics Society, IECON 2000*, Oct. 2000, pp. 387–392.

[2] I. Takahashi and T. Noguchi, "A new quick-response and high-efficiency control strategy of an induction motor," vol. IA-22, pp. 820–827, Sep./Oct. 1986.

[3] A. D. Cheok and Y. Fukuda, "A new torque and flux control method for switched reluctance motor drives," *IEEE Trans. Power Electron.*, vol. 17, no. 4, pp. 543–557, Jul. 2002.

[4] R. Jeyabharath, P. Veena, and M. Rajaram, "A novel dtc strategy of torque and flux control for switched reluctance motor drive," in *International Conference on Power Electronics, Drives and Energy Systems, PEDES 06*, Dec. 2006, pp. 1–5.

[5] H. J. Guo, “Considerations of direct torque control for switched reluctance motors,” in *Proceedings of the 2006 IEEE International Symposium on Industrial Electronics, ISIE 2006*, Jul. 2006, pp. 2321–2325.

[6] *VisualDSP++ 4.5, C/C^{++} compiler and library, Manual for ADSP-21xxx DSPs*, Analog Devices Inc, 2006.